

A germline GFP transgenic axolotl and its use to track cell fate: Dual origin of the fin mesenchyme during development and the fate of blood cells during regeneration

Lidia Sobkow^{a,*}, Hans-Henning Epperlein^b, Stephan Herklotz^a,
Werner L. Straube^a, Elly M. Tanaka^{a,*}

^a Max Planck Institute of Molecular Cell Biology and Genetics, Pfotenhauerstrasse 108, 01307 Dresden, Germany

^b Department of Anatomy, Fetscherstr. 74, TU Dresden, 01307 Dresden, Germany

Received for publication 14 June 2005, revised 22 November 2005, accepted 22 November 2005

Available online 4 January 2006

Abstract

The development of transgenesis in axolotls is crucial for studying development and regeneration as it would allow for long-term cell fate tracing as well as gene expression analysis. We demonstrate here that plasmid injection into the one-cell stage axolotl embryo generates mosaic transgenic animals that display germline transmission of the transgene. The inclusion of *SceI* meganuclease in the injections (Thermes, V., Grabher, C., Ristoratore, F., Bourrat, F., Choulika, A., Wittbrodt, J., Joly, J.S., 2002. *I-SceI* meganuclease mediates highly efficient transgenesis in fish. *Mech. Dev.* 118, 91–98) resulted in a higher percentage of F0 animals displaying strong expression throughout the body. This represents the first demonstration in the axolotl of germline transmission of a transgene. Using this technique we have generated a germline transgenic animal expressing GFP ubiquitously in all tissues examined. We have used this animal to study cell fate in the dorsal fin during development. We have uncovered a contribution of somite cells to dorsal fin mesenchyme in the axolotl, which was previously assumed to derive solely from neural crest. We have also studied the role of blood during tail regeneration by transplanting the ventral blood-forming region from GFP+ embryos into unlabeled hosts. During tail regeneration, we do not observe GFP+ cells contributing to muscle or nerve, suggesting that during tail regeneration blood stem cells do not undergo significant plasticity.

© 2005 Elsevier Inc. All rights reserved.

Keywords: Axolotl; Transgenesis; GFP; *I-SceI* meganuclease; Regeneration; Fin; Blood

Introduction

The production of transgenic animals is a powerful tool used successfully in many animal systems to study early embryogenesis, organogenesis and adult tissues. It is a particularly important technique for studying regeneration, as it would allow for long-term cell fate tracing, as well as gene expression analysis, two important aspects of understanding regeneration on a mechanistic level. Vertebrate regeneration is studied in several different model organisms, including caudata (salamanders) such as *Ambystoma mexicanum* (axolotl), anurans such as *Xenopus laevis*, and teleosts such as *Danio rerio*

(zebrafish) and *Oryzias latipes* (medaka). Each of these systems has distinct features for studying regeneration and these distinctions make it crucial to have transgenic and genomic resources available in each of the organisms. For example, *Xenopus* is able to regenerate its limbs and tails as a tadpole but then loses this capacity upon metamorphosis while salamanders retain the ability to regenerate a wide variety of tissues and structures including muscle, cartilage, skin, spinal cord, lens and jaw throughout their lifespan (Goss, 1969). A number of molecular and cellular aspects of regeneration are also distinctive. In particular, wider plasticity of cell differentiation is observed during regeneration in caudata such as the axolotl compared to *Xenopus*. Implantation and lineage tracing experiments have shown that in caudates, dedifferentiation of multinucleated muscle fibers into proliferative mononucleate cells contributes a significant number of cells to the blastema

* Corresponding authors. Fax: +49 351 210 1489.

E-mail addresses: sobkow@mpi-cbg.de (L. Sobkow), tanaka@mpi-cbg.de (E.M. Tanaka).

(Echeverri et al., 2001; Kumar et al., 2000; Lo et al., 1993). Furthermore, in vivo tracing of spinal cord cells revealed that neural progenitors have the potential to switch fate and form muscle and cartilage during tail regeneration (Echeverri and Tanaka, 2002a). Such metaplasia was not observed in *Xenopus* cell tracking experiments where each tissue layer exclusively regenerated itself (Gargioli and Slack, 2004). While teleosts are able to regenerate their fins and portions of the heart, complete regeneration of the spinal cord, as observed in axolotls, is not possible in most teleost species (Kawakami et al., 2004). On a cellular level the plasticity of cell differentiation during teleost regeneration has not yet been widely established.

Work in *Xenopus laevis* provides an excellent example of how transgenesis can be used for studying regeneration. The Cre-loxP system was used to trace muscle cell fate during tail regeneration where it was concluded that muscle fibers do not dedifferentiate (Gargioli and Slack, 2004; Ryffel et al., 2003). Gargioli and Slack also grafted embryonic tissue from GFP+ *Xenopus* embryos into unlabelled hosts to follow the fate of other tissue types and found no transdifferentiation of spinal cord and notochord cells during tail regeneration. To address the molecular pathways involved in initiating regeneration Beck et al. (2001, 2003) created transgenic animals where key extracellular and intracellular signaling molecules were under the control of the *Xenopus* HSP70 promoter, allowing induction of gene expression at the time of tail amputation. This work implicated a role of the Notch and BMP pathways in induction of tail regeneration. These *Xenopus* studies illustrate the value of transgenic approaches for regeneration research.

As the cellular and molecular differences between tail regeneration in anurans and caudata become more evident, the significance of studying regeneration in both taxa is becoming increasingly clear. It is, therefore, of particular importance to develop transgenic approaches in caudata. Two transgenic approaches have been described for the newt, *Cynops pyrrhogaster*. Makita et al. (1995) found that injection of fertilized *Cynops* eggs with a linearized eukaryotic expression vector containing the *lacZ* gene resulted in mosaic reporter gene expression in tailbud stage embryos. The inclusion of newt satellite 2 sequences in the plasmid augmented the extent of expression 10-fold, with a widespread distribution of gene expression in hatching larvae. Germline transmission was not assessed in these experiments. In a different approach, Ueda et al. (2005) successfully applied a modification of the *Xenopus* transgenic technique involving in vitro fertilization coupled to sperm injection to produce transgenic *Cynops pyrrhogaster*. Transgenic animals were generated at a frequency of approximately 2% and displayed uniform transgene expression throughout the body. Unfortunately, a disadvantage of the *Cynops* system is the complex life cycle and long time to sexual maturity, making propagation of transgenic lines unwieldy. Furthermore, in the Ueda protocol, a large number of females were required to produce enough unfertilized eggs for a single experiment, making the possibility of producing multiple transgenic lines difficult.

To circumvent these problems, we endeavored to produce germline transgenic animals in the axolotl (*Ambystoma*

mexicanum), a species that is easily bred under laboratory conditions with a generation time of approximately 1 year. Another advantage of using axolotls is the availability of skin pigment mutants such as the *white* mutant where pigment cells are inhibited from migrating out laterally under the epidermis from their neural crest origin on top of the neural tube (Epperlein and Lofberg, 1990). These mutants facilitate visualization of lineage tracers such as GFP in regeneration studies (Echeverri and Tanaka, 2002b, 2003). Our goal was to establish an efficient transgenesis method for the axolotl that would allow first, production of a large number of transgenic animals in the F0 generation and second, germline transmission. Due to the complications of applying the *Xenopus* protocol to caudate eggs, described in Ueda et al. (2005), we chose to test transgenesis protocols that are widely used in teleosts. Transgenesis in teleosts is normally achieved via direct injection of plasmid DNA into the fertilized egg. This results in F0 animals expressing the transgene in a mosaic fashion, a proportion of which display germline transmission of the transgene (Culp et al., 1991; Stuart et al., 1988, 1990). It was recently reported that coinjection of *ISceI* meganuclease with plasmids bearing its recognition sites enhances expression, decreases mosaicism in the F0 generation, and increases the germline transmission rate (Thermes et al., 2002). Here, we describe plasmid injection into the one-cell stage axolotl embryo as a method of generating transgenic animals and the evaluation of *ISceI* meganuclease's ability to enhance expression. Using this technique we report for the first time in the axolotl germline transmission of a transgene in a Mendelian ratio.

The availability of a GFP transgenic animal is a valuable reagent for cell tracking experiments, since it provides an indelible marking system with high spatial resolution that is visible in live animals. These animals provide a transplantation system comparable to the valuable quail-chick chimeras, which have been crucial for studying cell fate during avian embryogenesis and organogenesis (Le Douarin and Kalcheim, 1999). The axolotl is a particularly good system for tracking cell fate by transplanting tissues from a GFP+ animal into unlabeled hosts due to its unrivaled accessibility for tissue engraftment at any stage of its lifecycle. The transplantation of GFP+ cells circumvents the problems of other labeling techniques such as DiI, where the possibility of the dye spreading to unwanted cells always exists, or mRNA/dextran injection and electroporation which are relatively transient markers that are diluted out upon cell division. Here, we use embryonic tissue grafting to study two essential problems in development and regeneration. By transplantation of neural folds and somites, we demonstrate that the dorsal fin mesenchyme, which was originally assumed to derive entirely from neural crest (see Tucker and Slack, 2004), has a dual origin; deriving from both neural crest and from somites. Second, we examine the issue of hematopoietic cell plasticity and its contribution to regeneration. Recent reports of hematopoietic cells being able to contribute to other tissue lineages such as muscle or brain in the mouse have raised

controversy (Brazelton et al., 2000; Ferrari and Mavilio, 2002; Ferrari et al., 1998; Mezey et al., 2000). The frequency of such events, as well as their potential relevance to tissue regeneration is still open to question. We wanted to test whether blood cells display widespread plasticity during axolotl tail regeneration—namely whether blood cells contribute significantly to muscle and central nervous system. Here we do not observe blood cells contributing to muscle or central nervous system during tail regeneration, indicating that hematopoietic cell plasticity is not an ubiquitous mechanism used during regeneration.

Materials and methods

Animal care, embryo handling and injection protocol

All axolotls were bred and raised in the laboratory. In all experiments, white mutant (d/d) axolotls were used. Axolotls were staged according to the normal tables from (Bordzilovskaya et al., 1989). In all injection experiments embryos were used at the one-cell stage. Embryos were collected in the morning and kept in tap water at 4°C until the time of injection to assure they remained at the one-cell stage. All embryos were dejellied manually with fine forceps (Dumont 5, Fine Science Tools, Germany) and kept in 1× MMR with penicillin–streptomycin (Invitrogen GmbH, Germany). Our experience in embryo handling allows us to say that careful manual dejelling does not harm embryos and has very little effect on survival. However, since different spawns of embryos had differing survival rates, one part of each spawn was left as a quality and viability control. Control, non-dejellied, embryos were kept in aerated water.

Prior to injection embryos were transferred to chilled 20% Ficoll/1× MMR/pen-strep. (Ficoll obtained from Sigma, Germany). Injections were performed at the one-cell stage (at 22°C, the time from fertilization to the first division is 6 h; (Bordzilovskaya et al., 1989). Injections were performed using a pressure injector Picospritzer II (Parker Instrumentation) mounted alongside of an Olympus Stereo SZX12 dissecting microscope. Glass capillary needles were prepared on a Flaming/Brown micropipette puller; model P-97, (Sutter Instruments Co., USA). Needles were back-filled with DNA alone or DNA + ISceI Enzyme (DNA: 0.1 µg/µl or 0.01 µg/µl; ISceI enzyme: 1 U/µl; 1× meganuclease buffer. Enzyme and buffer were obtained from New England Biolabs, USA). 10 nl of solution was injected into the one-cell stage embryo. The optimal injection volume of 10 nl was established by a series of plasmid injections in the range of volumes from 30 nl to 5 nl. A volume of 20 nl can be used, however it may result in a lower survival rate of embryos depending on their quality. After injection embryos were kept in 20% Ficoll/1× MMR solution for 2–3 h to prevent yolk leakage and then were transferred to 5% Ficoll/0.1× MMR/pen-strep and left in this solution overnight. Finally, embryos were transferred to 0.1× MMR/pen-strep, until the hatching stage, when animals were kept in aerated tap water at room temperature. All solutions used for injections and embryo rearing were 0.22 µm filtered.

Grafting GFP+ neural folds and somites

Before being used for grafting white mutant (d/d) GFP+ donor embryos and white hosts were washed thoroughly with tap water and sterile Steinberg solution (Steinberg, 1975) containing antibiotics. They were then decapsulated manually. For grafting GFP+ trunk neural fold material or somites, GFP+ donors and hosts were placed into the depression of an agar dish filled with cold Steinberg saline. Grafting was performed under sterile conditions using tungsten needles.

Neural folds

Neural folds containing cranial and trunk regions ($n = 2$), or one complete left trunk neural fold ($n = 8$) were grafted orthotopically from white GFP+ transgenic neurulae (stages 15–17) into white mutant hosts from which neural fold material of equivalent size had been extirpated. Two to 4 days after the operation the distribution of GFP+ cells in the hosts was followed under fluorescence optics.

Somites

For grafting single somites, the epidermis was lifted from the left dorsolateral midtrunk of white GFP+ transgenic embryos (stages 23/24). One somite was extirpated and implanted into a similar site of a white host where a somite had been removed. The epidermis was then folded back over the implanted somite and pressed against it with a small glass disc for a few minutes. Migration of GFP+ cells into the dorsal fin was followed under fluorescence optics.

Histology and immunofluorescence

Several days after grafting GFP+ tissues larvae were anaesthetized with MS 222 (Serva) and fixed with 4% paraformaldehyde (PFA) in 0.1 M PBS overnight. Fixed specimens were washed and transverse vibratome sections (100 µm) were cut on a vibratome series 1000 sectioning system (Ted Pella, Inc.) in order to investigate the internal distribution of GFP+ cells. Some PFA-fixed larvae of similar age as larvae with GFP+ somites (stage 38) were embedded in paraffin (Leica ASP 300) for investigating the distribution of PAX7 positive dermatome cells on transverse sections (5 µm). Microwaved transverse sections (5 µm) were stained with a primary PAX7 antibody (DSHB) and with biotinylated secondary antibodies and tertiary streptavidin–peroxidase complexes (Vectastain ABC-Elite-Kit).

In the samples for characterizing the fully GFP transgenic animal, 5-day blastemas of GFP+ juveniles were fixed in 4% PFA overnight at 4°C, washed 3 × 15 min with PBS at room temperature and placed in 30% sucrose in PBS overnight at 4°C. Tails were mounted in Tissue Tek (Sakura) and cryosections (10 µm) were collected on Histobond Adhesion microslides (Marienfeld, Germany). To visualize the structure of the tissues, sections were stained with a hematoxylin solution (Sigma, Germany) for 20 s and washed extensively with tap water, followed by a 3-min wash in PBS. Nuclei were stained for 8 min with Hoechst followed by 3 × 5 min washes in PBS. Slides were mounted using Mowiol and allowed to dry overnight.

Microscopy

For transgene expression analysis animals were anesthetized with 0.001% ethyl-*p*-aminobenzoate (Sigma, Germany), placed on a coverslip and imaged using a 10× Plan-Neofluor objective on a Zeiss Axiovert 2 microscope with a CCD camera (Diagnostic Instruments, USA) controlled by a Metamorph image acquisition system (Visitron). For imaging of dissected GFP+ organs and tissues we used an Olympus Stereo SZX12 microscope with fluorescence attachment controlled by Diagnostic Instruments software (USA). Sections of GFP+ tissues from transgenic GFP animals were imaged on an Olympus BX61 microscope using brightfield and fluorescence optics.

Plasmid constructs

Plasmid constructs used in experiments were: pCSKA-hGFP-*SceI* (5.0 kb) (kindly provided by C. Grabher) that contains the *Xenopus borealis* cytoskeleton actin promoter driving hGFP flanked by *SceI* sites. CMVGFP3-ITR (5.3 kb). pCS2nβgalITR was digested with *HindIII* and *XhoI* to remove the *lacZ* sequence, which was replaced by the GFP3 sequence obtained after *HindIII/XhoI* digestion of XCarGFP3ITR. GFP3 is a version of GFP that was mutated for better expression in *Xenopus* (both plasmids used for this cloning—kind gift from Sylvia Evans).

pCAGGsEGFP(*Sce*) (5.9 kb) was constructed by insertion of two oligonucleotides containing *ISceI* recognition sequences in opposite orientations flanking the pCAGGsEGFP cassette that contains EGFP driven by chicken β-actin promoter with CMV-IE (CAGGsEGFP plasmid kindly provided by F. Stewart).

Plasmids were purified using MaxiPrep Kits (Quiagen, Germany) (pCSKA-hGFP-*SceI*, pCAGGsEGFP(*SceF*) and CMVGFP3-ITR), EndoFree Quiagen Kit (pCAGGsEGFP and pCAGGsEGFP(*Sce*)) and cesium chloride preparation (pCAGGsEGFP(*Sce*)). The type of plasmid purification in meganuclease injections did not seem to have a significant influence on expression or survival.

Table 1

Comparison of expression levels, duration of expression and survival rate of animals injected with three different promoters: CMV—cytomegalovirus promoter, CSKA—*X. borealis* cytoskeletal actin promoter, CAGGs—chicken b-actin promoter combined with IE CMV enhancer

Promoter	Survived/ injected (%)	Rate of expression % (No.)	Categories of expression at hatchling			Duration and intensity of EGFP expression in time			
			Very strong No./% survivors	Strong No./% survivors	Moderate No./% survivors	Weak No./% survivors	Embryo	Hatchling	Larvae (2 months)
CMV	113/639 (18)	34% (38)				38 (100)	++	+	–
CSKA	10/180 (6)	50% (5)			2 (40)	3 (60)	++	+	+
CAGGs	6/51 (12)	100% (6)	1 (17)	5 (83)			+++	+++	+++

The *ISceI* meganuclease enzyme (NEB, Germany) was aliquoted and stored at -80°C and used according to the teleost protocol available by personal communication with Jochen Wittbrodt and Clemens Grabher (Jochen.Wittbrodt@EMBL.de or Clemens.Grabher@EMBL.de).

Results

Plasmid injection results in mosaic transgene expression with the duration of expression being promoter dependent

To assess the efficacy of plasmid injection for generating stable transgene expression, we tested plasmids harboring three different constitutive promoters driving green fluorescent protein: cytomegalovirus (CMVGFP), *X. borealis* cytoskeletal actin (CSKAhGFP; Thermes et al., 2002), and cytoplasmic actin fused to the CMV enhancer, (CAGGsEGFP; Niwa et al., 1991). In this experiment we injected 2 ng of DNA/egg. All plasmids yielded mosaic expression of fluorescent protein in the developing embryos ranging from the labeling of an occasional cell, to animals where at least 50% of the body cells expressed the transgene.

To evaluate and compare the extent of mosaicism and intensity of expression we categorized the hatchlings into four expression categories (Table 1). “Very strong” indicated animals that displayed almost ubiquitous expression of GFP so that under the stereomicroscope the intensity of fluorescence was relatively uniform and distinct patches of cells were not visible. The “strong” category denoted animals where expression was widespread and strong, but some mosaicism was evident, with clearly visible patches of muscle, skin, heart, blood cells, veins, neural system and notochord. “Moderate” denoted animals with a weaker intensity of fluorescence in greater than 50% of the cells or animals with a higher intensity of fluorescence in slightly less than 50% of cells. Such animals typically expressed the reporter gene mostly in body muscles and skin and with very few blood cells and heart labeled. The “weak” category represented weak expression of reported gene and was mostly limited to small patches of body muscles and scattered patches of skin. From these observations it was clear that the intensity and extent of expression was promoter dependent (Table 1).

Significantly, the different promoters showed widely different persistence of expression over the course of development. The expression driven by the CMV promoter decreased steeply over time to the stage where all animals lost most of the fluorescent labeling by 2 months and only small, scattered groups of muscle or skin cells continued to

express label (Table 1). The CSKA promoter, although a cellular promoter, was also mildly silenced over time. In contrast, the expression obtained from the CAGGs promoter was strong and most importantly this strong expression persisted beyond 6 months (Figs. 1A and B). The one F0 male that displayed “very strong” GFP expression in close to all cells of the body was grown for 14 months to sexual maturity. Expression of GFP was stable throughout development and into adulthood (Figs. 1A and B). Considering the persistence of the CAGGs-driven expression, it is likely that the CMV-driven construct is silenced in the genome over time. Indeed delivery of CMV promoter driven constructs into rat muscle via adenovirus injection is extensively silenced soon after delivery to the cell (Brooks et al., 2004). Silencing of CMV-promoter driven gene expression has also been described in transgenic *Xenopus* (Ryffel et al., 2003). In contrast the CAGGs promoter has been used for widespread expression in transgenic mice (for

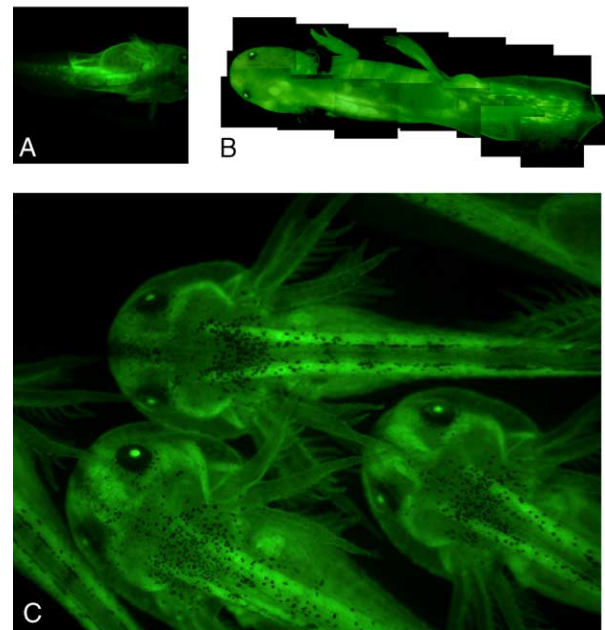


Fig. 1. Axolotl injected with CAGGsEGFP construct—founder animal of our first transgenic line of axolotl. CAGGs—chicken B-actin + IE CMV promoter. (A) Expression of EGFP after 1 month. The animal is about 1.2 cm long. (B) Expression of EGFP in the same animal after 6 months. The animal is about 13 cm long. Expression at this level was observed until the first mating. (C) F1 animals derived from mating of the GFP+ axolotl. Progeny are at the 2-cm-long larval stage. GFP is ubiquitously expressed all over the body.

Table 2
Embryos at one-cell stage were injected with various combinations of plasmid and *I-SceI* enzyme

Construct	Injected No.	Survived No./%	Very strong No./% survivors	Strong No./% survivors	Moderate No./% survivors	Weak No./% survivors
CAGGS GFP SCE + E	281	92 (33%)	15 (16%)	9 (10%)	31 (34%)	37 (40%)
CAGGS GFP SCE	157	74 (47%)	0	8 (11%)	23 (31%)	43 (58%)
CAGGS GFP + E	291	68 (23%)	0	3 (4%)	9 (13%)	56 (82%)
CAGGS GFP	223	61 (27%)	1 (2%)	3 (5%)	14 (23%)	43 (70%)
E	155	103 (66%)				

The quality of expression was checked after 1.5 months and animals were classified in categories of expression described in the text; E—*I-SceI* meganuclease enzyme.

example: (Okabe et al., 1997), and our results confirm its effectiveness in promoting ubiquitous expression in transgenic animals.

Coinjection of ISceI meganuclease enzyme with a plasmid containing its recognition sites enhances transgene expression

One goal was to develop a transgenesis method where we could produce relatively large numbers of animals with the least mosaicism possible in the F0 generation so that the F0 animals might be used directly in cell tracking experiments, as is done in *Xenopus*. A second consideration was germline transmission of the transgene. To reduce mosaicism in the F0 generation and to increase the chance of germline transmission we tested a method successfully implemented in medaka involving coinjection of *ISceI* enzyme mixed with plasmid containing its recognition sites (Thermes et al., 2002). *ISceI* meganuclease is an intron-encoded homing endonuclease with an 18 bp long recognition sites that was isolated from *S. cerevisiae* (Jacquier and Dujon, 1985). The meganuclease enzyme induces double stranded break formation at its recognition sites and probably also takes part in double strand break repair (Rouet et al., 1994).

To test whether the *ISceI* method alleviates mosaicism, we constructed a pCAGGs-EGFP plasmid where *SceI* sites flanked the expression cassette and injected the pCAGGsEGFP(*Sce*) and pCAGGsEGFP plasmids with and without enzyme. In initial experiments we tested optimal plasmid and enzyme concentrations by a series of plasmid injections in the range from 2 ng to 500 pg per embryo. Optimal results were obtained with injection of 1 ng of plasmid per embryo. With this amount of plasmid the optimal enzyme amount was established by series of injections where the enzyme concentration was varied from 0.01 to 4 U/ μ l. 1 U/ μ l (10 nU/embryo) of enzyme in the injection mix yielded optimal results. Co-injection of pCAGGs-EGFP(*Sce*) with the *ISceI* enzyme resulted in 16% of animals classified as “very strong” (Sup. Fig. 1) in comparison to the control injections where only 2% of animals were in this class (Table 2).

Germline transmission of transgene expression

To evaluate germline transmission we raised 15 F0 animals harboring the pCAGGsGFP plasmid to adulthood and performed matings with the white mutant. This experiment was performed prior to obtaining the animals from the meganuclease

experiments described above. Therefore, the animals used for mating represented one male with “very strong” expression, and 14 animals with “moderate or strong” expression (Sup. Fig. 1). In such matings, 6 out of 15 animals produced at least some GFP+ embryos in the F1 generation, with 3 animals generating over 20% GFP+ eggs (Table 3 and Sup. Fig. 1).

Notably, the mating of the “very strong” male depicted in Fig. 1 with a white female produced clutches where 50% of the eggs were GFP+. This result suggested that in this case, the transgene might be expressed from a single chromosome in all germ cells, resulting in Mendelian inheritance of the transgene. To confirm this ratio, this male was used for a second mating, resulting again in 50% eggs GFP+, supporting the notion of Mendelian inheritance of the transgene. In the eggs from these matings, GFP expression was first observed after the mid-blastula transition (stage 8 of development) consistent with zygotic expression of the GFP transgene from the male chromosome.

Fig. 1C depicts the GFP+ F1 transgenic animals at the larval stage. The animals appear to express GFP uniformly throughout their body. To examine in more detail whether the GFP transgene was ubiquitously expressed in the F1 animals various tissues from an F1 transgenic animal were compared to those from a white animal of the same age. Strong, ubiquitous GFP expression was observed in dissected forelimbs, eyes, hearts, lungs and livers (Fig. 2). Due to our interest in tail regeneration

Table 3
Germline transmission of pCAGGsEGFP

Animal	Sex (M/F)	No of EGFP+ embryos	No of EGFP– embryos	% embryos GFP+
1 (very strong)	M	160	150	52
2	F	159	213	43
3	F	0	150	0
4	F	0	183	0
5	F	10	163	6
6	M	3	311	1
7	F	0	46	0
8	M	0	62	0
9	F	0	207	0
10	M	0	175	0
11	F	8	493	1
12	F	0	59	0
13	F	0	80	0
14	M	40	152	21
15	M	0	243	0

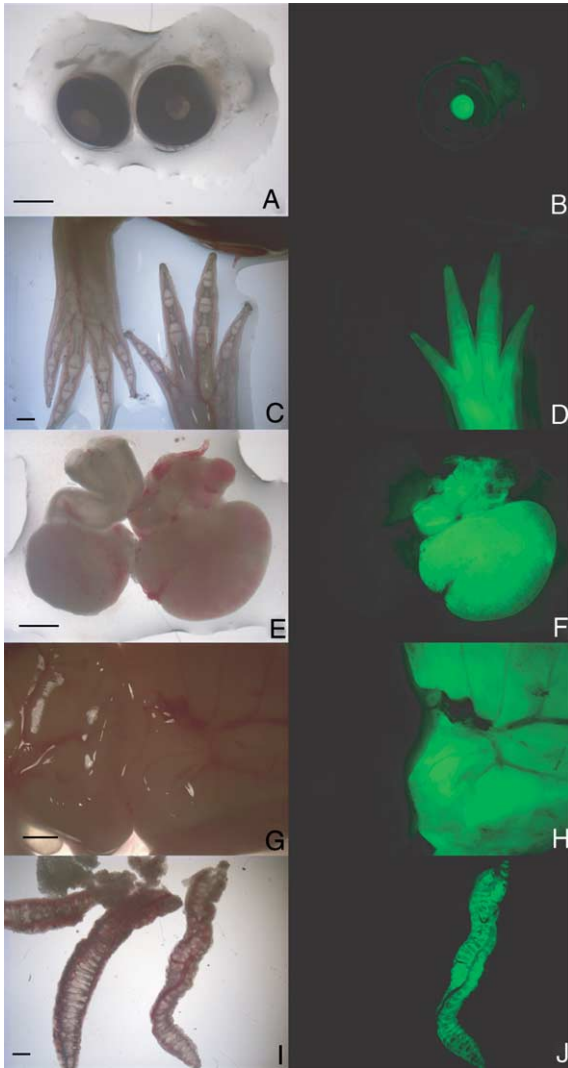


Fig. 2. GFP fluorescence of major organs and structures in GFP-transgenic compared to a non-transgenic animal. A and B shows comparison of eyes, C, D forelimbs, E, F heart, G, H liver, I, J lung. On figures A, C, E, G, I brightfield and on B, D, F, H, J fluorescent images are shown. Scale bars: A, B, C, D, E, F, I, J—1 mm, G, H—2 mm.

and blastema formation we examined GFP expression at higher resolution in longitudinal cryosections of regenerating tails (Figs. 3A–C). All tissues including mature and regenerating spinal cord (SC), the notochord (N), epidermis (E), and the blastema (B) were uniformly GFP+. By examining cells at high resolution in the tail fin (Figs. 3D–F) and the tail blastema (Figs. 3G–I), we could ascertain that all identifiable Höchst-positive cells were also GFP+. This is particularly clear in the dorsal tail fin where individual cells are widely separated from each other and embedded in a dense extracellular matrix (Figs. 3D–F). One exception to the ubiquitous expression was found in erythrocytes, which did not exhibit GFP fluorescence. A possible explanation was the quenching of GFP fluorescence by hemoglobin. Western blots on erythrocytes, however, showed that erythrocytes contained no detectable GFP protein. It thus appears that the erythrocyte differentiation program which involves general transcriptional inhibition (Walmsley et al., 1991) resulted in suppression of GFP expression.

Somite and neural crest contribute to dorsal fin mesenchyme

An animal constitutively expressing GFP is a valuable tool for analyzing the fate of cells during development and regeneration by grafting GFP+ cells into unlabeled hosts. The axolotl is particularly amenable to such an approach as tissues at all stages (embryonic, larval, juvenile and adult) engraft from one animal to another extremely well with no evidence of rejection. Here we have used grafting of GFP+ tissues to study cell fate during embryogenesis and regeneration. We have focused on the formation of the dorsal fin during embryogenesis, and the contribution of blood-derived cells to tail regeneration.

We were interested in the genesis and composition of the dorsal fin mesenchyme since it is a structure that contributes to tail regeneration but has been little studied. The fin mesenchyme is composed of stellate cells embedded in a dense extracellular matrix (Figs. 3D, E, F). In lower vertebrates, the mesenchyme of the dorsal fin has been classically assumed to be completely neural crest-derived (Du Shane, 1935; Raven, 1931, for schematic, see Tucker and Slack, 2004). To confirm the neural crest origin of dorsal fin mesenchyme, we replaced trunk neural folds (8 cases) and cranial folds in addition to trunk neural folds (2 cases) with GFP+ tissue at stage 16 and examined whether the dorsal fin was homogeneously labeled (Fig. 4A). Surprisingly, only the apical portions of the dorsal fin epidermis (stages 40–41) were GFP+ in all larvae (Fig. 4B). Transverse vibratome sections (4 individuals) showed that only half of the internal fin mesenchyme cells were GFP+ and also demonstrated the complete and specific labeling of the neural crest (Fig. 4C). These results suggested a possible additional non-neural crest contribution to the dorsal fin mesenchyme.

A hint to a potential additional source of dorsal fin mesenchyme came from PAX7 immunohistochemistry of stages 39–40 animals. In addition to the expected immunostaining in the dorsal neural tube (but not in the neural crest nor neural crest derived structures such as dorsal root ganglia), PAX7+ cells were observed in the dermatome (Fig. 4D) as well as some cells in the dorsal fin mesenchyme (Fig. 4D). This raised the possibility that the dermatome may contribute mesenchyme to the dorsal fin. To test this, we grafted GFP+ somites into unlabeled hosts at stage 23, well before neural crest has delaminated and migrated from the neural tube (Fig. 4E). Six out of seven larvae (stage 42) displayed GFP+ cells in the dorsal fin that sometimes populated even the apical-most regions of the fin (Figs. 4F, G). Transverse sections revealed that labeled cells were localized within the mesenchyme (Fig. 4H). As expected, no GFP+ neural crest derivatives were found in such grafted animals, confirming the specificity of the transplant. These experiments indicate that dorsal fin mesenchyme derives not only from neural crest but also significantly from the dermatome of the somites.

The contribution of blood cells to tail regeneration

In the following experiments we have used embryonic transplantation of the blood anlage in order to label blood in

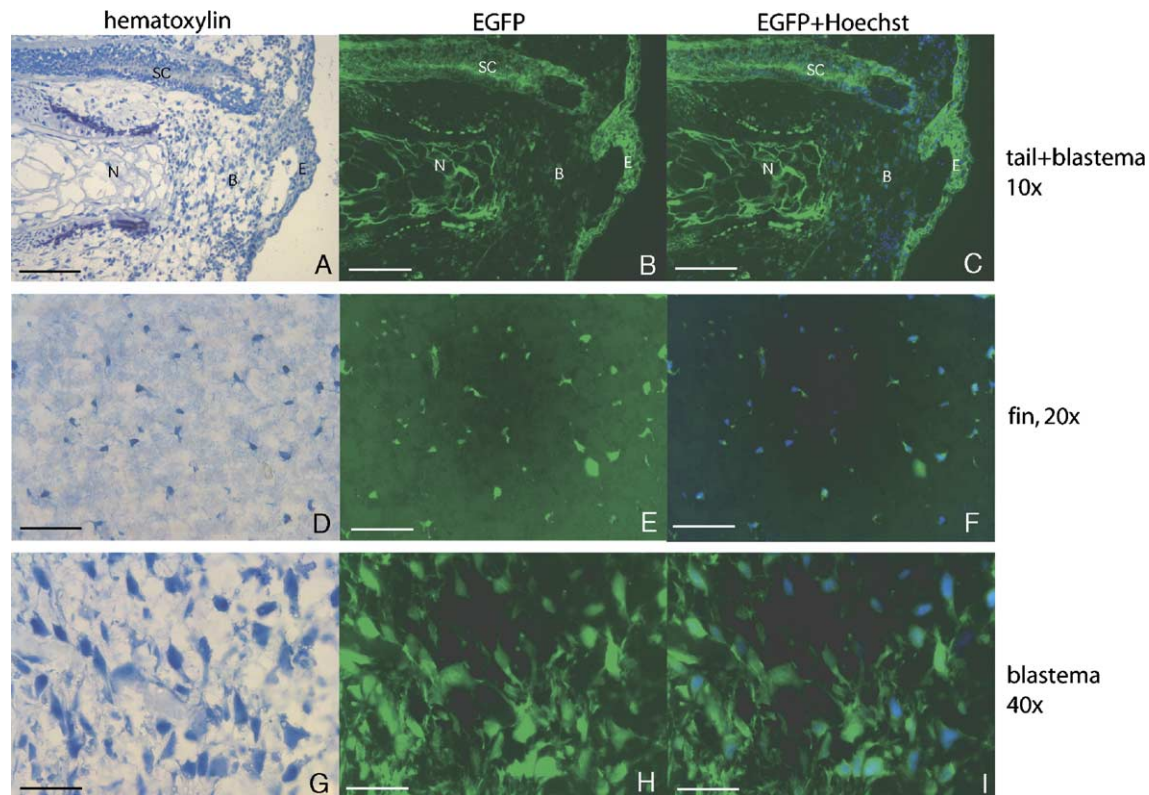


Fig. 3. High-resolution images of GFP fluorescence in cryosections of a regenerating axolotl tail. A regenerating tail of a transgenic fluorescent animal was sectioned longitudinally and stained with hematoxylin to visualize cells and H \ddot{o} chst to visualize nuclei. (A, B, C) An overview of the tail tissues. sc—spinal cord, n—notochord, b—blastema, e—epidermis. (D, E, F) Higher magnification view of tail fin cells. Note in hematoxylin and H \ddot{o} chst staining that cells are widely separated from each other via ECM. All cells are GFP+. (G, H, I) High magnification view of tail blastema cells. All H \ddot{o} chst positive cells are GFP+. (A, D, G) Hematoxylin staining. (B, E, H) GFP fluorescence from transgenic animal, (C, F, I) overlay of GFP and H \ddot{o} chst staining. Scale bars: A–C, 200 μ m; D–F, 100 μ m; G–I, 50 μ m.

the developing axolotl larvae, so that we could track the fate of blood cells during tail regeneration. At stage 18, we transplanted posterior ventrolateral mesodermal areas (with overlying epidermis) that will form the ventral blood islands (Fig. 6A) (Yamada, 1938). In urodeles, this region appears to be the major source of primitive and definitive hematopoiesis (Deparis and Jaylet, 1984; Durand et al., 2002). Of 30 transplants, 3 animals survived to 2 cm long larval stages where we could follow the course of tail regeneration. To estimate the percentage of circulating blood that derived from the GFP graft, we acquired blood samples from the fully GFP+ germline transgenic animals and compared it to blood from one of the grafted animals. In the fully transgenic animals, the erythrocytes were not GFP+ while the non-erythrocytic white blood cells were GFP+ resulting in 3.2% of the circulating blood cells being GFP+ in the fully transgenic animals. When we examined the blood from one of the grafted animals, 1% of the circulating blood was GFP+ indicating that we had labeled a significant proportion of the blood-forming region.

In the grafted animals, we could observe GFP+ cells in circulating blood (see supplementary movie), as well as GFP+ cells that were evenly distributed throughout the tail including the dorsal fin (Figs. 5B and C). The primary cell type that we observed labeled based on morphology, were Langerhans cells, which are dendritic cells primarily found in skin, dermis and lymph nodes. Fig. 5D and E show

Langerhans cells with their characteristic cell extensions. The occurrence of GFP+ cells containing melanin granules inside their cytoplasm (Fig. 5E) confirms that these are Langerhans cells that are processing skin antigens (for review see: Romani et al., 2003). We also observed other cells with a smaller, rounded to polygonal shape that are presumably macrophages and leukocytes (Fig. 5F) (Jones and Corwin, 1996). The presence of Langerhans cells and macrophages confirms that our transplants label myeloid lineages.

To determine the contribution of blood cells to regenerating tissues we amputated the grafted animals when they were 2 cm long larvae and allowed the tail to regenerate for 2 weeks (Fig. 6A). Each animal was amputated twice bringing the total number of observations to six. Tail amputation caused rapid blood efflux, followed within several minutes by the formation of a blood clot. After several hours, the blood clot was enclosed by the wound epidermis and became part of the blastema. One day post-amputation, we observed an accumulation of GFP+ cells close to the amputation plane, either as a result of blood clotting or due to the migration of GFP+ cells towards the wound (Fig. 6D). Analysis of the regenerated part of the tail within the first few days after the lesion shows that the GFP+ cells that appear in the regenerated tissue are similar in shape as those in the tail before the regeneration (Sup. Fig. 2). After 13 days, we observed the same even

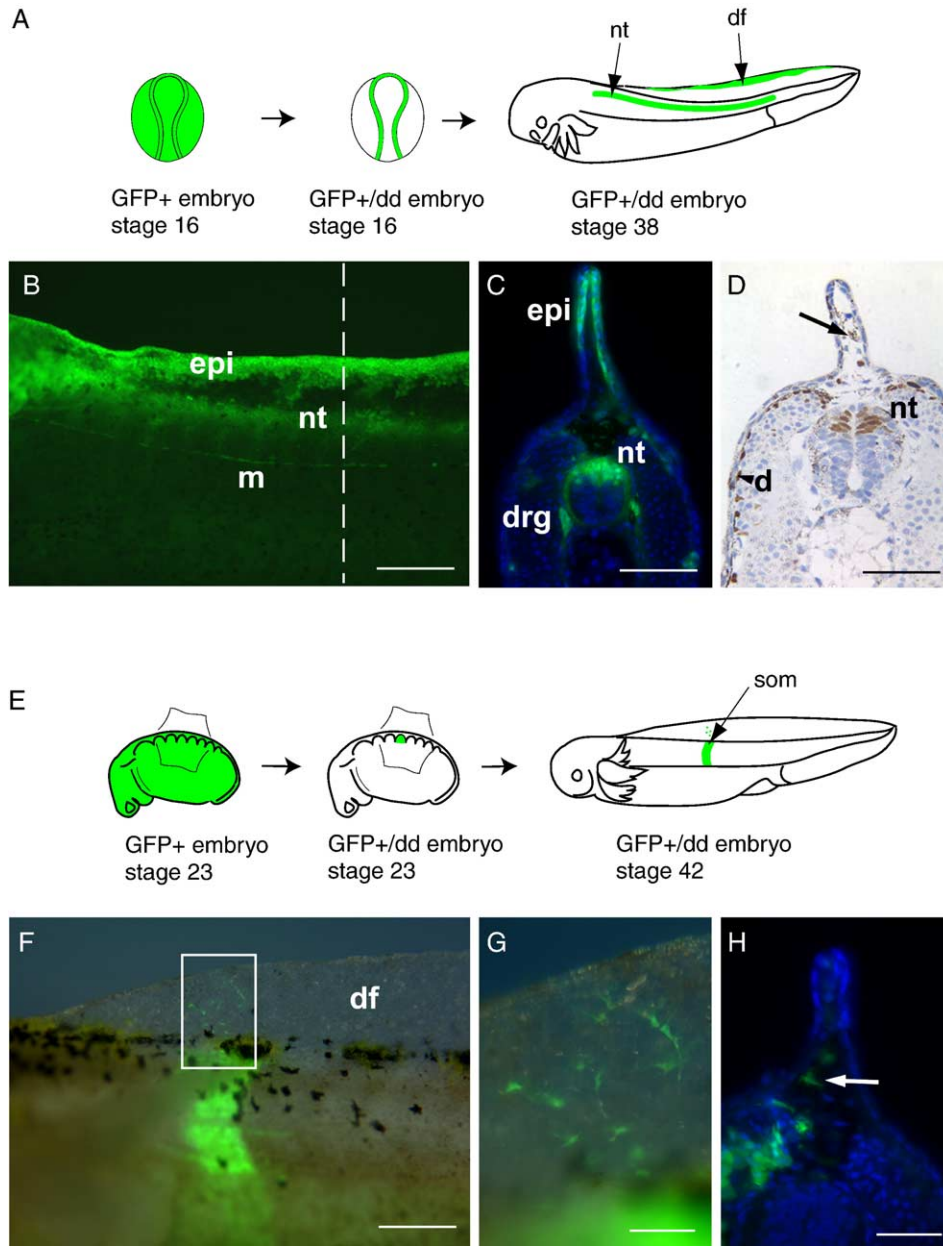


Fig. 4. Dual origin of dorsal fin mesenchyme. (A) Schematic showing grafting of GFP+ neural folds to unlabelled hosts in order to investigate the contribution of neural crest to the dorsal fin. Both cranial and trunk neural folds were labeled. (B) Left side of a white axolotl larva (head to the left, outside the image; stage 40–41) in which both cranial and trunk neural folds had been replaced with GFP+ neural folds as depicted in A. The label is visible in the apex of the dorsal fin epidermis (epi), the neural tube (nt) and the middle lateral line nerve (m). Dotted line denotes the level of transverse section shown in C. (C) Transverse vibratome section through the larva shown in B demonstrates labeling of the apical part of the dorsal fin epidermis (epi). Fin mesenchyme is only sparsely labeled. Higher magnification views showed approximately 50% of mesenchymal cells labeled (data not shown). Dorsal neural tube (nt) and dorsal root ganglia (drg) are stained. (D) Anti-PAX7 immunostaining of a transverse paraffin section through the trunk of a larva at stage 39–40. Cells in the dorsal neural tube (nt), dermatome (d) and dorsal fin mesenchyme (arrow) reacted positively. (E) Grafting of one, left, GFP+ mid-trunk somite to unlabelled host in order to investigate possible contribution of dermatome cells to dorsal fin mesenchyme. (F) Left side of a white axolotl larva (head to the left, outside the image; stage 40–41) in which one somite had been replaced with a GFP+ somite as described in E. GFP+ cells, very likely dermatome cells, have left the somite and have migrated into the dorsal fin (df; enlargement see G). (H) Transverse vibratome section through GFP+ somite revealing migrated GFP+ cells (arrows) within the dorsal fin mesenchyme. Scale bars: B, 250 μ m; C, D, F, H, 100 μ m; G, 50 μ m.

distribution of stellate GFP+ cells in the tail, with no contribution to muscle, cartilage or spinal cord (Fig. 6H, I). Transverse sections of the regenerated tail confirmed that the GFP+ cells were not located within muscle, cartilage or spinal cord tissue (data not shown).

Discussion

The ability to produce transgenic axolotls with relative ease opens up numerous opportunities for producing animals harboring other cell markers, and for manipulating gene

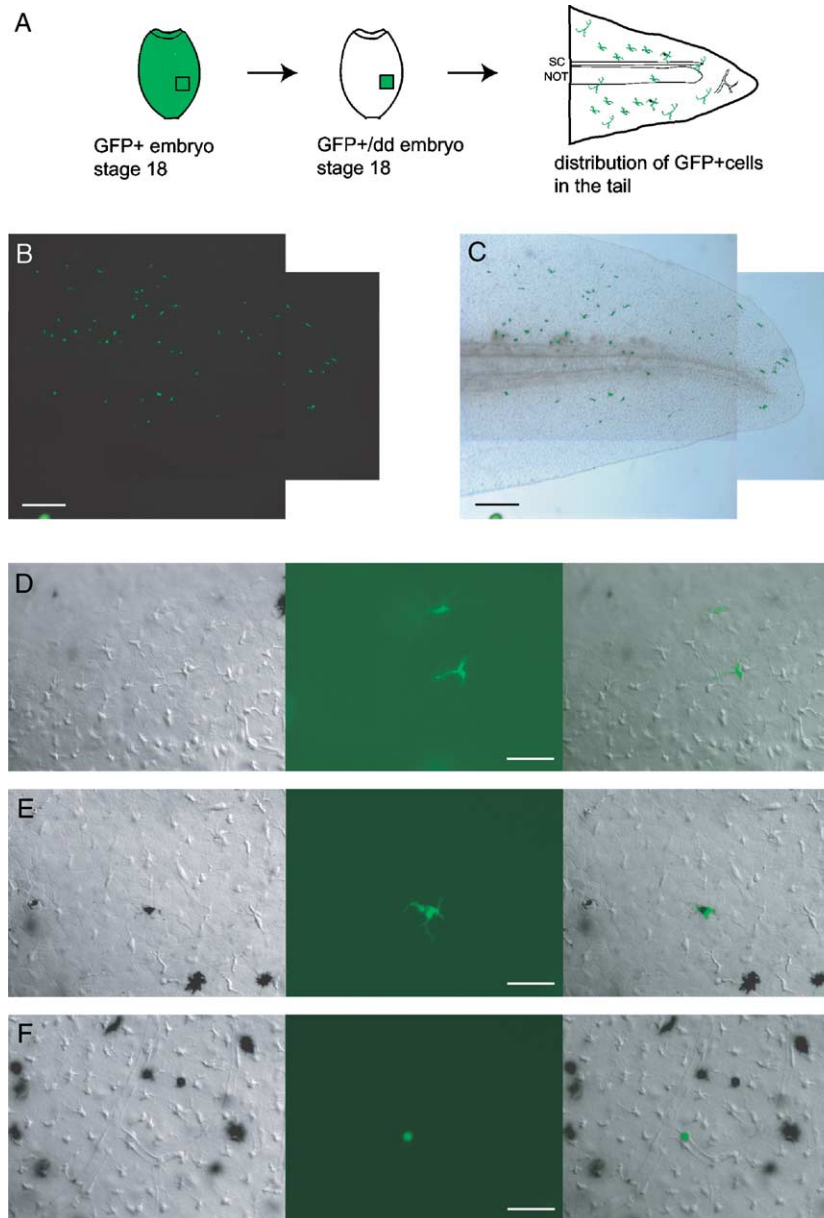


Fig. 5. Identification of GFP+ blood cell types in the mature tail after grafting GFP+ blood anlage to unlabelled hosts. (A) Schematic showing grafting of GFP+ ventro-lateral tissue at stage 18 to unlabelled hosts and the subsequent pattern of labeling observed in the tail. sc—spinal cord, not—notochord. (B) Fluorescent image of a tail derived from grafting experiments. (C) Overlay of fluorescence and bright field image. (D) High magnification images of a Langerhans cell in the dorsal fin; DIC, fluorescence and overlaid images. (E) High-magnification images of a Langerhans cell in the dorsal fin that has taken up melanin granules; DIC, fluorescence and overlaid images. (F) A second subtype of GFP+ cell that likely represents a macrophage; DIC, fluorescence and overlaid images. Scale bars: B, C, 0.5 mm; D, E, F, 50 μ m.

expression in the axolotl, an important dimension that was previously unavailable for this animal. As shown here, an important aspect is the differing temporal expression profiles of supposedly constitutive promoters, where expression from some promoters was lost over time. Further studies will be needed to determine whether a broad scope of promoters will be functional in these transgenics. In *Xenopus*, faithful tissue specific expression has been observed using promoters from heterologous species (Hartley et al., 2001). We expect that such promoters would display the same tissue specificity using the plasmid injection technique.

While a broader assessment of the transgenic technique regarding different promoters and transgenes is necessary work for the future, an emphasis of the work described here is the use of the GFP germline transgenic animal for cell tracking experiments during development and regeneration. These GFP+ animals are an important tool for embryological and regeneration experiments where specific cell or tissue types need to be followed over long periods of time. Previously, grafting experiments in axolotls were performed using either triploid nucleoli or skin pigment which all have major limitations for analysis (Muneoka et al., 1984;

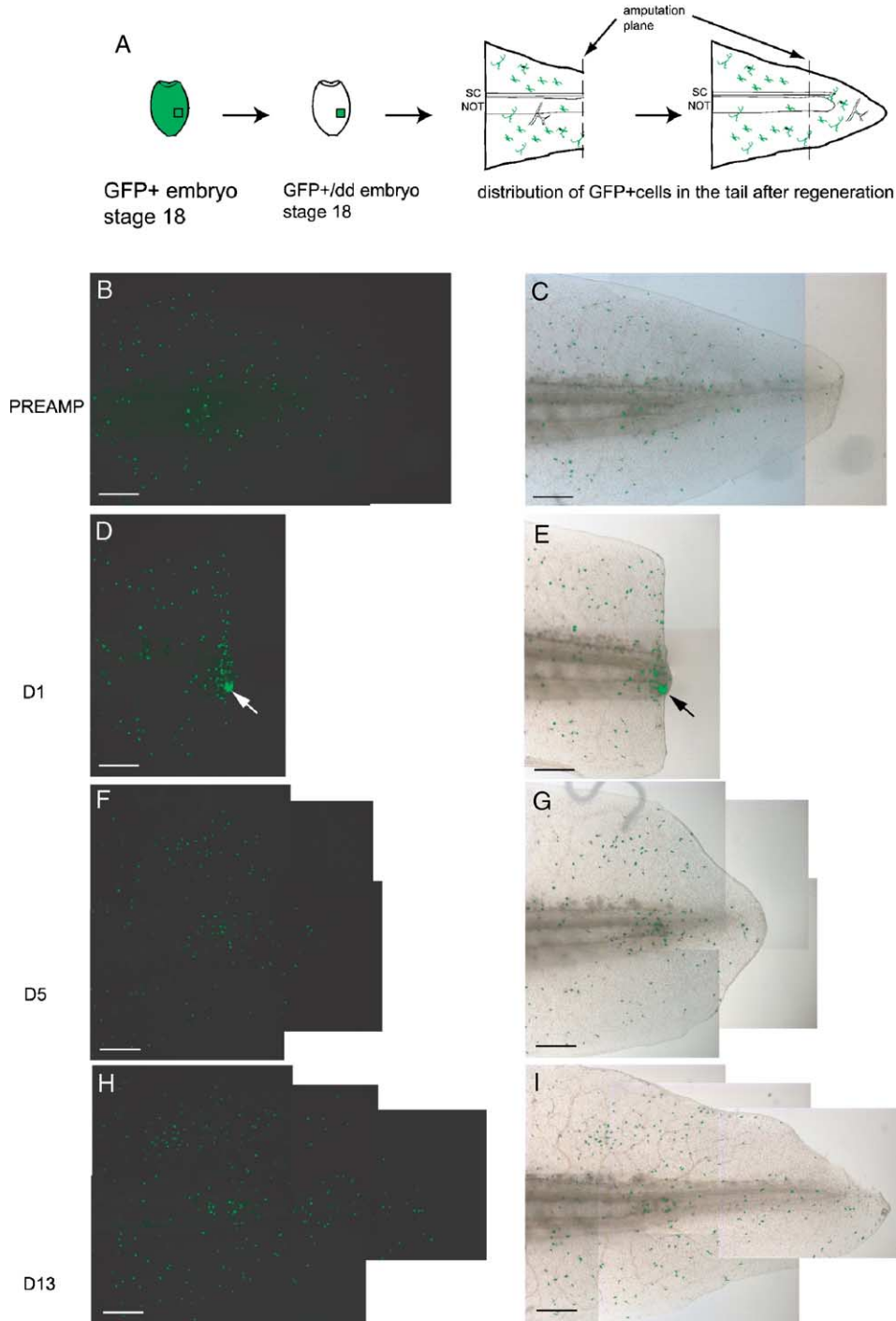


Fig. 6. Tail amputation of transplanted animals containing GFP+ blood cells. (A) Schematic showing grafting of GFP+ ventro-lateral tissue at stage 18 to unlabelled hosts and the subsequent pattern of labeling observed in the tail. After reaching a size of 1.5–2 cm animals were subjected to amputation and the contribution of GFP+ blood and its derivatives to the regenerated tail was followed over 13 days. sc—spinal cord, not – notochord. (B and C) Fluorescent and overlay images of the tail preamputation. (D and E) Fluorescent and overlay images respectively of the regenerated tail after 1 day. Arrow indicates group of cells embedded in the blood clot. (F and G) Regenerated tail after 5 days (fluorescence and overlay respectively). GFP+ cells have populated the growing blastema. (H and I) Almost fully regenerated tail after 13 days, where tail structures including spinal cord, cartilage and muscle have started differentiating. GFP+ cells populated the regenerated tail with a similar distribution as in the mature tissue. No labeling of muscle fibers, spinal cord or cartilage was observed. Scale bars: B–I, 0.5 mm.

Pescitelli and Stocum, 1980). The pigmentation grafts are only useful in grafts containing skin. In the triploid nucleoli technique only a proportion of the grafted cells contained three nucleoli and are distinguishable from host cells (Muneoka et al., 1984). Thus, there is no one-to-one correspondence of grafted cells to the marker. Secondly,

the grafts can only be analyzed upon fixation and histological analysis. In contrast, GFP+ tissue can be followed dynamically over time in live animals, and provides an indelible marker with high spatial resolution, as shown here in our studies of the dorsal fin, and of blood during regeneration.

Classical transplantation experiments demonstrated that neural crest cells contribute to the dorsal fin mesenchyme (Raven, 1931, 1936) and since that time it has been assumed that neural crest is the sole contributor of mesenchymal cells of the dorsal fin (see Bodenstein, 1952; Tucker and Slack, 2004). Our experiments where we transplant complete GFP⁺ neural folds indicated that only approximately 50% of the dorsal fin mesenchyme came from neural crest. Transplantation of GFP⁺ somites at stage 23 resulted in GFP⁺ dorsal fin mesenchyme, indicating that somites (presumably dermatome) also contribute cells to the dorsal fin mesenchyme. In light of our new findings, it is possible to re-interpret Bodenstein's (1952) transplantation results as being consistent with a dual, neural crest and somite origin of dorsal fin mesenchyme. Bodenstein transplanted prospective dorsal fin epidermis laterally over somites at stage 28 and observed the formation of a proper dorsal fin containing mesenchymal cells. He interpreted this result as indicating that the neural crest cells that had migrated out of the neural tube and populated the somites had contributed to the ectopic dorsal fin mesenchyme. Our somite transplantations were performed well before neural crest delamination and migration which start in the anterior trunk at stages 28 and 31, respectively, (Epperlein and Lofberg, 1990), eliminating the possibility that the somite-derived fin mesenchyme derives from migrating neural crest. In a second set of experiments, Bodenstein transplanted dorsal tissue that included ectoderm and the dorsal half of the neural tube to the ventral midline in order to observe if these two cell layers were sufficient to form dorsal fin at an ectopic site. The ectopic fins that formed were approximately half the size of the normal fin. When the same dorsal tissue pieces were transplanted over somites, full sized fins formed. In a third set of experiments, when dorsal tissue that included ectoderm, neural tube and somites were transplanted into the ventral midline, full-sized fin structures formed. Thus, there was a strong association of full-sized fin formation with the presence of somites. Our experiments here indicate that this is due to a major contribution of somites to dorsal fin mesenchyme.

An important question for the future is whether the contribution of somites to fin mesenchyme is a feature specific to urodele amphibians or whether it is generally found in all lower vertebrates with fins. Smith et al. (1994) used Dil labeling to characterize the source of fin mesenchyme in zebrafish. Labeling of neural crest resulted in labeled cells in the dorsal fin mesenchyme, while labeling of somites did not. At this point, it is unclear whether this difference to our results is due to a difference in fin formation between species, or to a technical difference in the experiments.

Here we have also used embryonic transplantation of GFP⁺ blood anlage to test the frequency and role of hematopoietic cell plasticity during tail regeneration. By transplanting the embryonic blood-forming region, it is possible to label blood cells, including the stem cells that give rise to hematopoietic cells. The axolotl may be an ideal model system for such experiments, since it is thought that the blood (primitive and definitive) derives solely or largely from the ventral blood islands rather than from additional dispersed sites (Durand et al., 2002). Since the tail is distant from the blood-forming region in the main

body, a large graft of the ventral body tissue does not interfere with the specificity of visualizing blood in the tail.

So far, we have observed no contribution of labeled blood cells to muscle or central nervous system, as was reported in the mouse (Brazelton et al., 2000; Ferrari et al., 1998; Mezey et al., 2000). It is difficult to compare quantitatively the frequency of cell type switching occurring in the mouse with our results. During the course of our experiments we estimate that we have tracked in total approximately 600 GFP⁺ blood-derived cells (non-circulating), but the total number of stem cells, for example, that we are tracking is unknown. Comparison of GFP⁺ cells in circulating blood in the germline transgenic animals versus a grafted animal indicated that we had labeled up to 30% of the total blood cell population.

Our results indicating that blood cells do not contribute significantly to regenerating tissues is consistent with classical irradiation experiments performed to determine whether the regenerating limb blastema arises locally from cells at the amputation plane, or from distant cells (such as circulating blood cells) that would home to the injury site (Butler and O'Brien, 1942). In these experiments, a segment of the left hindlimb was exposed to X-irradiation while the rest of the body was shielded. When the limb was amputated in the exposed region regeneration did not occur, while amputation through the shielded regions did result in regeneration. These experiments indicated that the main proportion of cells involved in limb regeneration arise from the tissue at the amputation plane. Our results coupled with the Butler and O'Brien work indicate that although hematopoietic cells may have the potential to form distant cell types, this plasticity is not utilized or required for regeneration of complex structures such as the limb or tail. Our results would thus imply that a more important issue for understanding regeneration is how tissues at the injury site such as muscle, dermis and nerve are induced to produce the progenitor cells of the blastema.

Acknowledgments

We would like to acknowledge the dedicated contribution of Heino Andreas to the entire axolotl husbandry and thank D. De Pietri Tonelli and A. Tazaki for critical reading of the manuscript. We are grateful to Francis Stewart, Clemens Grabher, Jochen Wittbrodt for advice and reagents, and Sylvia Evans for constructs. This research was funded by grant I/78 766 from the Volkswagen Foundation.

Appendix A. Supplementary data

Supplementary data associated with this article can be found in the online version at [doi:10.1016/j.ydbio.2005.11.037](https://doi.org/10.1016/j.ydbio.2005.11.037).

References

- Beck, C.W., Whitman, M., Slack, J.M., 2001. The role of BMP signaling in outgrowth and patterning of the *Xenopus* tail bud. *Dev. Biol.* 238, 303–314.
- Beck, C.W., Christen, B., Slack, J.M., 2003. Molecular pathways needed for regeneration of spinal cord and muscle in a vertebrate. *Dev. Cell* 5, 429–439.

- Bodenstein, D., 1952. Studies on development of the dorsal fin in Amphibians. *J. Exp. Zool.* 120, 213–245.
- Bordzilovskaya, N.P., Dettlaff, T.A., Duhon, S.T., Malacinski, G.M., 1989. Developmental-Stage Series of Axolotl Embryos. Oxford Univ. Press, New York.
- Brazelton, T.R., Rossi, F.M., Keshet, G.I., Blau, H.M., 2000. From marrow to brain: expression of neuronal phenotypes in adult mice. *Science* 290, 1775–1779.
- Brooks, A.R., Harkins, R.N., Wang, P., Qian, H.S., Liu, P., Rubanyi, G.M., 2004. Transcriptional silencing is associated with extensive methylation of the CMV promoter following adenoviral gene delivery to muscle. *J. Gene Med.* 6, 395–404.
- Butler, E.G., O'Brien, J.P., 1942. Effects of localized x-irradiation on regeneration of urodele limb. *Anat. Rec.* 84, 407–413.
- Culp, P., Nusslein-Volhard, C., Hopkins, N., 1991. High-frequency germ-line transmission of plasmid DNA sequences injected into fertilized zebrafish eggs. *Proc. Natl. Acad. Sci. U. S. A.* 88, 7953–7957.
- Deparis, P., Jaylet, A., 1984. The role of endoderm in blood cell ontogeny in the newt *Pleurodeles waltl*. *J. Embryol. Exp. Morphol.* 81, 37–47.
- Du Shane, G.P., 1935. An experimental study of the origin of pigment cells in Amphibia. *J. Exp.*, 19.
- Durand, C., Kerfoum, F., Charlemagne, J., Fellah, J.S., 2002. Identification and expression of Helios, a member of the Ikaros family, in the Mexican axolotl: implications for the embryonic origin of lymphocyte progenitors. *Eur. J. Immunol.* 32, 1748–1752.
- Echeverri, K., Tanaka, E.M., 2002a. Ectoderm to mesoderm lineage switching during axolotl tail regeneration. *Science* 298, 1993–1996.
- Echeverri, K., Tanaka, E.M., 2002b. Mechanisms of muscle dedifferentiation during regeneration. *Semin. Cell Dev. Biol.* 13, 353–360.
- Echeverri, K., Tanaka, E.M., 2003. Electroporation as a tool to study in vivo spinal cord regeneration. *Dev. Dyn.* 226, 418–425.
- Echeverri, K., Clarke, J.D., Tanaka, E.M., 2001. In vivo imaging indicates muscle fiber dedifferentiation is a major contributor to the regenerating tail blastema. *Dev. Biol.* 236, 151–164.
- Epperlein, H.H., Lofberg, J., 1990. The development of the larval pigment patterns in *Triturus alpestris* and *Ambystoma mexicanum*. *Adv. Anat., Embryol. Cell Biol.* 118, 1–99.
- Ferrari, G., Mavilio, F., 2002. Myogenic stem cells from the bone marrow: a therapeutic alternative for muscular dystrophy? *Neuromuscul. Disord.* 12 (Suppl. 1), S7–S10.
- Ferrari, G., Cusella-De Angelis, G., Coletta, M., Paolucci, E., Stornaiuolo, A., Cossu, G., Mavilio, F., 1998. Muscle regeneration by bone marrow-derived myogenic progenitors. *Science* 279, 1528–1530.
- Gargioli, C., Slack, J.M., 2004. Cell lineage tracing during *Xenopus* tail regeneration. *Development* 131, 2669–2679.
- Goss, R.J., 1969. Principles of Regeneration. Academic Press.
- Hartley, K.O., Hardcastle, Z., Friday, R.V., Amaya, E., Papalopulu, N., 2001. Transgenic *Xenopus* embryos reveal that anterior neural development requires continued suppression of BMP signaling after gastrulation. *Dev. Biol.* 238, 168–184.
- Jacquier, A., Dujon, B., 1985. An intron-encoded protein is active in a gene conversion process that spreads an intron into a mitochondrial gene. *Cell* 41, 383–394.
- Jones, J.E., Corwin, J.T., 1996. Regeneration of sensory cells after laser ablation in the lateral line system: hair cell lineage and macrophage behavior revealed by time-lapse video microscopy. *J. Neurosci.* 16, 649–662.
- Kawakami, A., Fukazawa, T., Takeda, H., 2004. Early fin primordia of zebrafish larvae regenerate by a similar growth control mechanism with adult regeneration. *Dev. Dyn.* 231, 693–699.
- Kumar, A., Velloso, C.P., Imokawa, Y., Brockes, J.P., 2000. Plasticity of retrovirus-labelled myotubes in the newt limb regeneration blastema. *Dev. Biol.* 218, 125–136.
- Le Douarin, N.M., Kalcheim, C., 1999. The Neural Crest. Second ed. Cambridge Univ. Press, Cambridge.
- Lo, D.C., Allen, F., Brockes, J.P., 1993. Reversal of muscle differentiation during urodele limb regeneration. *Proc. Natl. Acad. Sci. U. S. A.* 90, 7230–7234.
- Makita, R., Kondoh, H., Okamoto, M., 1995. Transgenesis of newt with exogenous gene expression facilitated by satellite 2 repeats. *Dev. Growth Differ.* 37, 605–616.
- Mezey, E., Chandross, K.J., Harta, G., Maki, R.A., McKercher, S.R., 2000. Turning blood into brain: cells bearing neuronal antigens generated in vivo from bone marrow. *Science* 290, 1779–1782.
- Muneoka, K., Wise, L.D., Fox, W.F., Bryant, S.V., 1984. Improved techniques for use of the triploid cell marker in the axolotl, *Ambystoma mexicanum*. *Dev. Biol.* 105, 240–245.
- Niwa, H., Yamamura, K., Miyazaki, J., 1991. Efficient selection for high-expression transfectants with a novel eukaryotic vector. *Gene* 108, 193–199.
- Okabe, M., Ikawa, M., Kominami, K., Nakanishi, T., Nishimune, Y., 1997. 'Green mice' as a source of ubiquitous green cells. *FEBS Lett.* 407, 313–319.
- Pescitelli Jr., M.J., Stocum, D.L., 1980. The origin of skeletal structures during intercalary regeneration of larval *Ambystoma* limbs. *Dev. Biol.* 79, 255–275.
- Raven, C.P., 1931. Zur Entwicklung der Ganglienleiste: I. Die Kinematik der Ganglienleistenentwicklung bei den Urodelen. *Wilhelm Roux' Arch. Entwicklunsmech. Org.* 125, 210–293.
- Raven, C.P., 1936. Zur Entwicklung der Ganglienleiste: V. Über die Differenzierung des Rumpfganglienleistenmaterials. *Wilhelm Roux' Arch. Entwicklunsmech. Org.* 134, 122–145.
- Romani, N., Holzmann, S., Tripp, C.H., Koch, F., Stoitzner, P., 2003. Langerhans cells—dendritic cells of the epidermis. *APMIS* 111, 725–740.
- Rouet, P., Smih, F., Jasin, M., 1994. Introduction of double-strand breaks into the genome of mouse cells by expression of a rare-cutting endonuclease. *Mol. Cell. Biol.* 14, 8096–8106.
- Ryffel, G.U., Werdien, D., Turan, G., Gerhards, A., Goosses, S., Senkel, S., 2003. Tagging muscle cell lineages in development and tail regeneration using Cre recombinase in transgenic *Xenopus*. *Nucleic Acids Res.* 31, e44.
- Smith, M., Hickman, A., Amanze, D., Lumsden, A., Thorogood, P., 1994. Trunk neural crest origin of caudal fin mesenchyme in the zebrafish *Brachydanio rerio*. *Proc. R. Soc. London* 256, 137–145.
- Steinberg, M.S., 1975. A nonnutrient culture medium for amphibian embryonic tissue. *Carnegie Inst. Washington, Year Book* 56, 347–348.
- Stuart, G.W., McMurray, J.V., Westerfield, M., 1988. Replication, integration and stable germ-line transmission of foreign sequences injected into early zebrafish embryos. *Development* 103, 403–412.
- Stuart, G.W., Vielkind, J.R., McMurray, J.V., Westerfield, M., 1990. Stable lines of transgenic zebrafish exhibit reproducible patterns of transgene expression. *Development* 109, 577–584.
- Thermes, V., Grabher, C., Ristoratore, F., Bourrat, F., Choulika, A., Wittbrodt, J., Joly, J.S., 2002. I-SceI meganuclease mediates highly efficient transgenesis in fish. *Mech. Dev.* 118, 91–98.
- Tucker, A.S., Slack, J.M., 2004. Independent induction and formation of the dorsal and ventral fins in *Xenopus laevis*. *Dev. Dyn.* 230, 461–467.
- Ueda, Y., Kondoh, H., Mizuno, N., 2005. Generation of transgenic newt *Cynops pyrrhogaster* for regeneration study. *Genesis* 41, 87–98.
- Walmsley, M.E., Buckle, R.S., Allan, J., Patient, R.K., 1991. A chicken red cell inhibitor of transcription associated with the terminally differentiated state. *J. Cell Biol.* 114, 9–19.
- Yamada, T., 1938. Der Determinationszustand des Rumpfmesoderms im Molchkeim nach der Gastrulation. *Roux's Arch.*, 137.